REPORT No. 759

DERIVATION OF CHARTS FOR DETERMINING THE HORIZONTAL TAIL LOAD VARIATION WITH ANY ELEVATOR MOTION

By HENRY A. PEARSON

SUMMARY

The equations relating the wing and tail loads are derived for a unit elevator displacement. These equations are then converted into a nondimensional form and charts are given by which the wing- and tail-load-increment variation may be determined under dynamic conditions for any type of elevator motion and for various degrees of airplane stability. In order to illustrate the use of the charts, several examples are included in which the wing and tail loads are evaluated for a number of types of elevator motion. Methods are given for determining the necessary derivatives from results of wind-tunnel tests when such tests are available.

INTRODUCTION

Because airplane failures in which tail surfaces were involved have occurred in flight, considerable impetus has been given to the task of setting up more rational methods of evaluating tail loads. Particular interest has been shown in the analysis of dynamic tail loads associated with more or less sudden elevator motions.

The problem of determining the dynamic tail loads in a rational manner has been treated by many authors. Various approaches and assumptions have been employed, but the methods available at present are too lengthy to be suitable for the routine computations that would have to be made in design studies. This statement is particularly true if the critical types of elevator motion are to be varied considerably from the simple types that have usually been treated. Although equations were given in reference 1 for determining the tail load with any variation of elevator motion, the equations were not in the best form for making computations. It has been found recently, as a result of a number of computations, not only that the method of reference 1 can be shortened but also that some of the minor factors which were previously omitted can now be included in a method that will be suitable for use by designers.

SYMBOLS

The following is a list of the symbols employed in this paper:

W	airplane weight, pounds
g	acceleration of gravity, feet per second^2
m	airplane mass, W/g, slugs
S	gross wing area including area within fuselage, square feet
S_t	gross horizontal-tail area including that intercepted by fuselage, square feet
b	wing span, feet
b_t	tail span, feet
k_Y	radius of gyration about pitching axis, feet
I	pitching moment of inertia, slug-feet square
x_t	length from center of gravity of airplane to aerodynamic center of tail (negative for conventional airplanes), feet
V	airplane velocity, feet per second
ρ	mass density of air, slugs per cubic foot
q	dynamic pressure, pounds per square foot $\left(\frac{1}{2}\rho V^2\right)$
η_t	tail efficiency factor (q_t/q)
L	lift, pounds
C_L	lift coefficient (L/qS)
M	moment, foot-pounds
C_m	pitching-moment coefficient of airplane without horizontal tail (Mb/qS^2)
α	wing angle of attack, radians
α_t	tail angle of attack, radians
i_t	tail setting, radians
δ	elevator angle, radians
ϵ	downwash angle, radians $\left(\frac{d\epsilon}{d\alpha}\alpha\right)$
γ	flight-path angle, radians
θ	angle of pitch $(\alpha+\gamma)$, radians
K	empirical constant denoting ratio of damping moment of complete airplane to damping moment of tail alone
n	airplane load factor
t	time, seconds
τ	aerodynamic time, unit$=m/\rho SV$
μ	airplane density ratio $(-m/\rho Sx_t)$
a, b	roots of basic differential equation when they are imaginary
m_1, m_2	roots of basic differential equation when they are real
K_1, K_2, K_3	dimensional constants occurring in basic differential equation
K_1', K_2', K_3'	nondimensional constants occurring in basic differential equation

The notations $\dot{\alpha}$ and $\ddot{\alpha}$, $\dot{\theta}$ and $\ddot{\theta}$, and so forth denote single and double differentiations with respect to either t or τ.

Subscripts:

0	initial or selected value
t	tail
max	maximum value
d	down
l_0	zero lift
geo	geometric

THEORETICAL RELATIONS BETWEEN WING AND TAIL LOAD

The mathematical treatment of the longitudinal motion of an airplane following an elevator displacement involves three simultaneous nonlinear differential equations. The correct analytical solution of these equations must be obtained either by a series substitution or by step-by-step methods. A close approximation to the correct solution is obtained if it is assumed that, in the interval between the start of the maneuver and the attainment of maximum loads

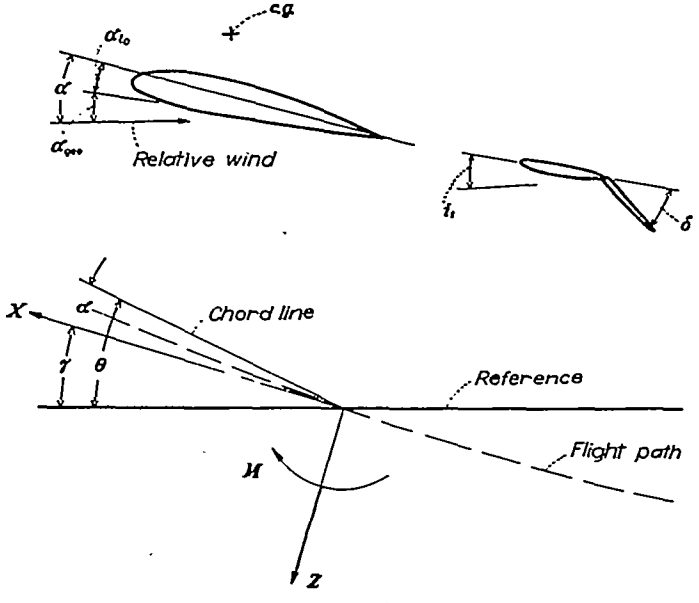

FIGURE 1.—Sign conventions employed. Positive directions shown.

on the wing and tail surfaces, neither the initial velocity nor the initial attitude changes materially. These assumptions eliminate one of the three equations of motion and the trigonometric coefficients that occur in the other two equations. In addition, the assumptions agree with experimental flight results and have been generally used in all treatments of the longitudinal motion of an airplane following a control deflection.

If the sign conventions of figure 1 are used, the following equations will apply to the steady flight condition

$$W\cos\gamma_0-\frac{dC_L}{d\alpha}\alpha_0 qS=0 \tag{1}$$

$$C_{m_0}q\frac{S^2}{b}+\frac{dC_{L_t}}{d\alpha_t}\left[\alpha_0\left(1-\frac{d\epsilon}{d\alpha}\right)+i_t+\frac{d\alpha_t}{d\delta}\delta_0\right](\eta_t q)S_t x_t=0 \tag{2}$$

Equation (1) represents the summation of the forces perpendicular to the instantaneous flight path and equation (2) represents the moments about the center of gravity.

In accordance with the assumption that there is no loss in speed during the pull-up, the corresponding dynamic equations can be written as

$$W\cos(\gamma_0+\Delta\gamma)-\frac{dC_L}{d\alpha}(\alpha_0+\Delta\alpha)qS$$
$$-\frac{dC_{L_t}}{d\delta}\eta_t qS_t\Delta\delta+m\dot\gamma V=0 \tag{3}$$

for the vertical forces. In this equation the term $\frac{dC_{L_t}}{d\delta}\eta_t qS_t\Delta\delta$ is introduced to allow for the change in the Z force that will occur with elevator deflection. If the slope $dC_L/d\alpha$ is used for the complete airplane with the tail surfaces in place and elevator fixed, most of the effect of the tail load on the vertical force will be taken into account.

The moment equation is

$$\left(C_m+\frac{dC_m}{d\alpha}\Delta\alpha\right)q\frac{S^2}{b}+\frac{dC_{L_t}}{d\alpha_t}\left[(\alpha_0+\Delta\alpha)\left(1-\frac{d\epsilon}{d\alpha}\right)\right.$$
$$\left.-\frac{\dot\alpha x_t}{V}\frac{d\epsilon}{d\alpha}-\frac{\dot\theta x_t}{V}\frac{K}{\sqrt{\eta_t}}+i_t+\frac{d\alpha_t}{d\delta}(\delta_0+\Delta\delta)\right]\eta_t qS_t x_t$$
$$+\frac{dC_{m_t}}{d\delta}\eta_t q\frac{S_t^2}{b_t}\Delta\delta-mk_Y^2\ddot\theta=0 \tag{4}$$

In equation (4) the term containing $\dot\alpha$ is introduced to correct for the effect of time lag in downwash at the tail, the term containing $\dot\theta$ is introduced to account for the change in tail angle due to rotation, and the term $\frac{dC_{m_t}}{d\delta}\eta_t q\frac{S_t^2}{b_t}\Delta\delta$ is introduced to account for the moment due to elevator camber. Computations have indicated that in some cases it is necessary to include both the camber term and the elevator-force term.

If equations (1) and (2) are subtracted from equations (3) and (4), respectively, and if it is assumed that only a small change in attitude takes place (so that $\cos(\gamma_0+\Delta\gamma)\cong\cos\gamma$), the following equations of motion are obtained

$$m\dot\gamma V-\frac{dC_L}{d\alpha}\Delta\alpha qS-\frac{dC_{L_t}}{d\delta}\eta_t qS_t\Delta\delta=0 \tag{5}$$

$$\frac{dC_m}{d\alpha}\Delta\alpha q\frac{S^2}{b}+\frac{dC_{L_t}}{d\alpha_t}\left[\Delta\alpha\left(1-\frac{d\epsilon}{d\alpha}\right)-\dot\alpha\frac{x_t}{V}\frac{d\epsilon}{d\alpha}-\dot\theta\frac{x_t}{V}\frac{K}{\sqrt{\eta_t}}\right.$$
$$\left.+\frac{d\alpha_t}{d\delta}\Delta\delta\right]\eta_t qS_t x_t+\frac{dC_{m_t}}{d\delta}\eta_t q\frac{S_t^2}{b_t}\Delta\delta-mk_Y^2\ddot\theta=0 \tag{6}$$

From figure 1 the following relations are seen to exist:

$$\begin{aligned}\theta&=(\alpha_0+\Delta\alpha)+(\gamma_0+\Delta\gamma)\\ \dot\theta&=\dot\alpha+\dot\gamma\\ \ddot\theta&=\ddot\alpha+\ddot\gamma\end{aligned} \tag{7}$$

Thus, from equations (5) and (7)

$$\dot{\gamma}=\dot{\theta}-\dot{\alpha}=\frac{dC_L}{d\alpha}\Delta\alpha q\frac{S}{mV}+\frac{dC_{L_t}}{d\delta}\eta_t q\frac{S_t}{mV}\Delta\delta \tag{8}$$

and

$$\dot{\gamma}=\theta-\ddot{\alpha}=\frac{dC_L}{d\alpha}\dot{\alpha}q\frac{S}{mV}+\frac{dC_{L_t}}{d\delta}\eta_t q\frac{S_t}{mV}\dot{\delta} \tag{9}$$

If equations (8) and (9) are substituted into equation (6), the terms containing $\ddot{\alpha}$, $\dot{\alpha}$, $\Delta\alpha$, $\dot{\delta}$, and $\Delta\delta$ are segregated and, if the resulting equation is divided by $-mk_Y^2=-I$, there is obtained

$$\ddot{\alpha}+\dot{\alpha}\left[\frac{dC_{L_t}}{d\alpha_t}\frac{S_t x_t^2}{2I}\rho\eta_t V\left(\frac{K}{\sqrt{\eta_t}}+\frac{d\epsilon}{d\alpha}\right)+\frac{dC_L}{d\alpha}\frac{\rho}{2}V\frac{S}{m}\right]$$

$$-\Delta\alpha\left[\frac{dC_m}{d\alpha}q\frac{S^2}{Ib}+\frac{dC_{L_t}}{d\alpha_t}(\eta_t q)\frac{S_t x_t}{I}\left(1-\frac{d\epsilon}{d\alpha}-\frac{dC_L}{d\alpha}\frac{K}{\sqrt{\eta_t}}\frac{\rho}{2}\frac{Sx_t}{m}\right)\right]=$$

$$\Delta\delta\left[\frac{dC_{L_t}}{d\delta}(\eta_t q)\frac{S_t x_t}{I}+\frac{dC_{m_t}}{d\delta}(\eta_t q)\frac{S_t^2}{Ib_t}-\frac{dC_{L_t}}{d\alpha_t}\frac{dC_{L_t}}{d\delta}\frac{K\eta_t^2}{\sqrt{\eta_t}}\frac{\rho}{2}\frac{x_t^2 S_t^2}{mI}q\right]$$

$$-\dot{\delta}\left[\frac{dC_{L_t}}{d\delta}\eta_t q\frac{S_t}{mV}\right] \tag{10}$$

The effect of the term containing $\dot{\delta}$ is small and may be omitted. Thus, equation (10) can be written as

$$\ddot{\alpha}+K_1\dot{\alpha}+K_2\Delta\alpha=K_3\Delta\delta \tag{11}$$

This equation is the equation for a damped oscillation with an impressed moment $K_3\Delta\delta$ where

$$K_1=\frac{\rho V}{2m}\left[\frac{dC_{L_t}}{d\alpha_t}\frac{S_t x_t^2}{k_Y^2}\eta_t\left(\frac{K}{\sqrt{\eta_t}}+\frac{d\epsilon}{d\alpha}\right)+\frac{dC_L}{d\alpha}S\right]$$

$$K_2=-\frac{\rho V^2}{2m}\left\{\frac{dC_m}{d\alpha}\frac{S^2}{k_Y^2 b}+\frac{dC_{L_t}}{d\alpha_t}\eta_t\frac{S_t x_t}{k_Y^2}\left[\left(1-\frac{d\epsilon}{d\alpha}\right)-\frac{dC_L}{d\alpha}\frac{K}{\sqrt{\eta_t}}\frac{\rho}{2}\frac{Sx_t}{m}\right]\right\}$$

$$K_3=\frac{\rho V^2}{2m}\left[\frac{dC_{L_t}}{d\delta}\eta_t\frac{S_t x_t}{k_Y^2}+\frac{dC_{m_t}}{d\delta}\eta_t\frac{S_t^2}{b_t k_Y^2}-\frac{dC_{L_t}}{d\alpha_t}\frac{dC_{L_t}}{d\delta}\frac{K\eta_t^2}{\sqrt{\eta_t}}\frac{\rho}{2}\frac{x_t^2 S_t^2}{mk_Y^2}\right] \tag{11a}$$

The increment in wing load, wing-load factor, and tail load can be found by solving equation (11) for $\Delta\alpha$ and $\dot{\alpha}$ by the usual methods. The increment in wing load and wing-load factor could then be obtained from the equations

$$\Delta L=\frac{dC_L}{d\alpha}\Delta\alpha qS$$

$$\Delta n=\frac{dC_L}{d\alpha}\frac{\Delta\alpha q}{W/S} \tag{12}$$

It is seen from the bracketed term in equation (6) that, in order to determine the effective tail angle of attack $\Delta\alpha_t$ at any time, the pitching velocity and the rate of change of the wing angle of attack must first be known. If substitutions are made from equations (7) and (8) into this bracketed term, the increment in effective tail angle of attack at any time is very closely given by the following equation

$$\Delta\alpha_t=\left[\Delta\alpha\left(1-\frac{d\epsilon}{d\alpha}-\frac{dC_L}{d\alpha}\frac{\rho}{2}\frac{\overrightarrow{S}}{m}\frac{x_t}{\sqrt{\eta_t}}\right)-\dot{\alpha}\frac{x_t}{V}\left(\frac{d\epsilon}{d\alpha}+\frac{1}{\sqrt{\eta_t}}\right)+\frac{d\alpha_t}{d\delta}\Delta\delta\right] \tag{13}$$

The value of $\Delta\alpha_t$ given in equation (13) is to be inserted in the equation

$$\Delta L_t=\frac{dC_{L_t}}{d\alpha_t}\Delta\alpha_t\eta_t qS_t \tag{14}$$

to obtain the tail-load increment at any time.

Up to this point the equations and method are straightforward and similar to the analysis previously presented in reference 1 with the exception that the rate of change of vertical force with elevator angle and the change in moment caused by tail camber have been introduced into the equations. These additional factors are usually small, but they tend to gain in importance as the amount of static stability is increased. For the case of a very stable airplane their contributions may affect the results in the order of about 5 to 10 percent.

The solution of the differential equation of motion (equation (11)) is not particularly difficult but would become rather tedious when the elevator motion is a complicated function of the time or when various types of elevator motion are to be considered. Also, in the form given, new computations would be required for each altitude and for each speed and the computations made for one airplane would not be applicable to another.

The first difficulty can be avoided by evaluating the results for a unit instantaneous elevator-angle change; then, since the equations are linear and the principle of superposition applies, Carson's or Duhamel's integral theorem may be used (see reference 2 for application) to obtain results for any assumed elevator variation. The second difficulty can be partly overcome by selecting, as did Glauert, new units of time and length and presenting charts for the unit solutions of $\Delta\alpha$ and $\dot{\alpha}$ for the various degrees of stability that would be obtained for center-of-gravity positions between the aerodynamic center and the stick-fixed neutral point.

In line with these ideas, the increment in elevator angle will be taken as unity and the unit of time, instead of being taken as 1 second, will be taken as $\tau=\frac{m}{\rho SV}$ seconds. The unit of length will be taken as x_t feet so that the unit of velocity will be $\frac{x_t}{\tau}$ or V/μ where $\mu=\frac{-m}{\rho Sx_t}$. Since x_t is a negative quantity, with the system of axes used, μ will be a positive quantity the value of which may range from about 10 to 100.

Introducing the above quantities into equation (11) allows a similar differential equation to be obtained, which can be written as

$$\ddot{\alpha}+K_1'\dot{\alpha}+K_2'\Delta\alpha=K_3'\Delta\delta(1) \tag{15}$$

where $\Delta\delta(1)$ is a unit displacement and

$$K_1'=\frac{1}{2}\left[\frac{dC_{L_t}}{d\alpha_t}\frac{S_t}{S}\frac{x_t^2}{k_Y^2}\eta_t\left(\frac{K}{\sqrt{\eta_t}}+\frac{d\epsilon}{d\alpha}\right)+\frac{dC_L}{d\alpha}\right]$$

$$K_2'=\frac{\mu}{2}\left\{\frac{dC_m}{d\alpha}\frac{S}{k_Y^2}\frac{x_t}{b}+\eta_t\frac{dC_{L_t}}{d\alpha_t}\frac{S_t}{S}\frac{x_t^2}{k_Y^2}\left[\left(1-\frac{d\epsilon}{d\alpha}\right)-\frac{dC_L}{d\alpha}\frac{K}{\sqrt{\eta_t}}\frac{\rho g}{2}\frac{Sx_t}{W}\right]\right\}$$

$$K_3'=-\frac{\mu}{2}\left[\frac{dC_{L_t}}{d\delta}\eta_t\frac{S_t}{S}\frac{x_t^2}{k_Y^2}+\frac{dC_{m_t}}{d\delta}\eta_t\frac{x_t}{b_t}\frac{S_t^2}{Sk_Y^2}-\frac{dC_{L_t}}{d\alpha_t}\frac{dC_{L_t}}{d\delta}\frac{K\eta_t^2}{\sqrt{\eta_t}}\frac{\rho}{2m}\frac{x_t^3S_t^2}{Sk_Y^2}\right] \tag{15a}$$

The value of K_1' is always positive and the value of K_2' is positive if the center of gravity lies ahead of the rear neutral point. The rear neutral point is defined here as the position along the mean aerodynamic chord at which the center of gravity would have to be in order that the slope of the moment curve for the *complete* airplane about this point be 0. The value of $dC_m/d\alpha$ that is used in this report is taken about a forward neutral point (with tail off), which has been called the aerodynamic center. The quantity K_3' is always negative and depends only on the geometric and aerodynamic qualities of the tail.

The solution of equation (15) can take any one of three forms, depending on whether both roots of the auxiliary equation are real and unequal (m_1, m_2), real and equal ($m_1=m_2$), or imaginary in the form of $a\pm ib$. With the stipulation that the center of gravity be forward of the rear neutral point, the motion indicated by equation (15) always subsides and the solutions for $\Delta\alpha$ and $\dot{\alpha}$ are as follows:

Unequal real roots $m_1\neq m_2$

$$\Delta\alpha=\frac{K_3'\delta(1)}{K_2'}\left\{1-\frac{e^{-\frac{K_1'}{2}\tau}}{\sqrt{\left(\frac{K_1'}{2}\right)^2-K_2'}}\left[\frac{K_1'}{2}\sinh\left(\sqrt{\left(\frac{K_1'}{2}\right)^2-K_2'}\right)\tau+\sqrt{\left(\frac{K_1'}{2}\right)^2-K_2'}\cosh\left(\sqrt{\left(\frac{K_1'}{2}\right)^2-K_2'}\right)\tau\right]\right\} \tag{16}$$

$$\dot{\alpha}=\frac{K_3'\delta(1)}{\sqrt{\left(\frac{K_1'}{2}\right)^2-K_2'}}e^{-\frac{K_1'\tau}{2}}\sinh\left(\sqrt{\left(\frac{K_1'}{2}\right)^2K_2'}\right)-\tau$$

Equal real roots $m_1=m_2$

$$\Delta\alpha=\frac{K_3'\delta(1)}{K_2'}\left[1-e^{-\frac{K_1'}{2}\tau}\left(\frac{K_1'\tau}{2}+1\right)\right]$$

$$\dot{\alpha}=\frac{K_3'\delta(1)}{K_2'}\left[\left(\frac{K_1'}{2}\right)^2\tau e^{-\frac{K_1'}{2}\tau}\right] \tag{16a}$$

Imaginary roots $a\pm ib$

$$\Delta\alpha=\frac{K_3'\delta(1)}{K_2'}\left\{1+e^{-\frac{K_1'}{2}\tau}\left[\frac{-K_1'}{2\sqrt{K_2'-\left(\frac{K_1'}{2}\right)^2}}\sin\left(\sqrt{K_2'-\left(\frac{K_1'}{2}\right)^2}\right)\tau-\cos\left(\sqrt{K_2'-\left(\frac{K_1'}{2}\right)^2}\right)\tau\right]\right\}$$

$$\dot{\alpha}=\frac{K_3'\delta(1)e^{-\frac{K_1'}{2}\tau}}{\sqrt{K_2'-\left(\frac{K_1'}{2}\right)^2}}\sin\left[\sqrt{K_2'-\left(\frac{K_1'}{2}\right)^2}\right]\tau \tag{16b}$$

In these solutions, the boundary conditions are at $\tau=0$, $\Delta\alpha=\dot{\alpha}=0$, $\Delta\delta(1)=1.0$. References to equations (5) and (7), however, indicate that the boundary conditions should be at $\tau=0$, $\Delta\alpha=0$, $\Delta\delta(1)=1.0$, $\dot{\theta}=0$, so that $\dot{\alpha}=-\dot{\gamma}=\frac{dC_L}{d\delta}\frac{S_t}{S}\frac{\eta_t}{2}$. The inclusion of these conditions complicates the solution and introduces factors that prevent the presentation of results in a few basic charts. Actual plots of the unit-solution curves obtained with either boundary condition indicate, in examples that have been tried, such small differences that the two curves can be hardly distinguished. For these reasons, the simple boundary conditions have been used.

It has been found by direct substitution that the value of K_1' will range from about 5 to 9 in the case of conventional airplanes. (See equation (15a).) Similar substitutions for K_2' indicate that this quantity may range from about 2 to about 300 when all possible values of μ and ρ are considered. There are, however, compensating factors that enter into the problem so that the likely range of K_2' is much smaller than this even when the possible present-day extremes of the separate items are considered.

CHARTS FOR DETERMINING $\Delta\alpha$ AND $\dot{\alpha}$

Charts are given in figures 2 to 6 showing the variation of $\Delta\alpha\frac{K_2'}{K_3'}$ and $\frac{\dot{\alpha}}{K_3'}$ against aerodynamic time τ for all values of K_1' and K_2' that are likely to occur. The charts given apply as long as K_2' remains a positive quantity, which will always be the case when there is a small margin of static stability, namely, when the center of gravity is ahead of the rear neutral point. According to the bracketed term of equation (15a), the center of gravity could be slightly behind the neutral point and the motion given by equation (15) would still subside because of the greater stability which the airplane has on a curved path.

USE OF THE CHARTS IN A TYPICAL EXAMPLE

In order to illustrate the generality of the charts given in figures 2 to 6, an example is worked for a typical fighter airplane which is now under investigation for tail loads.

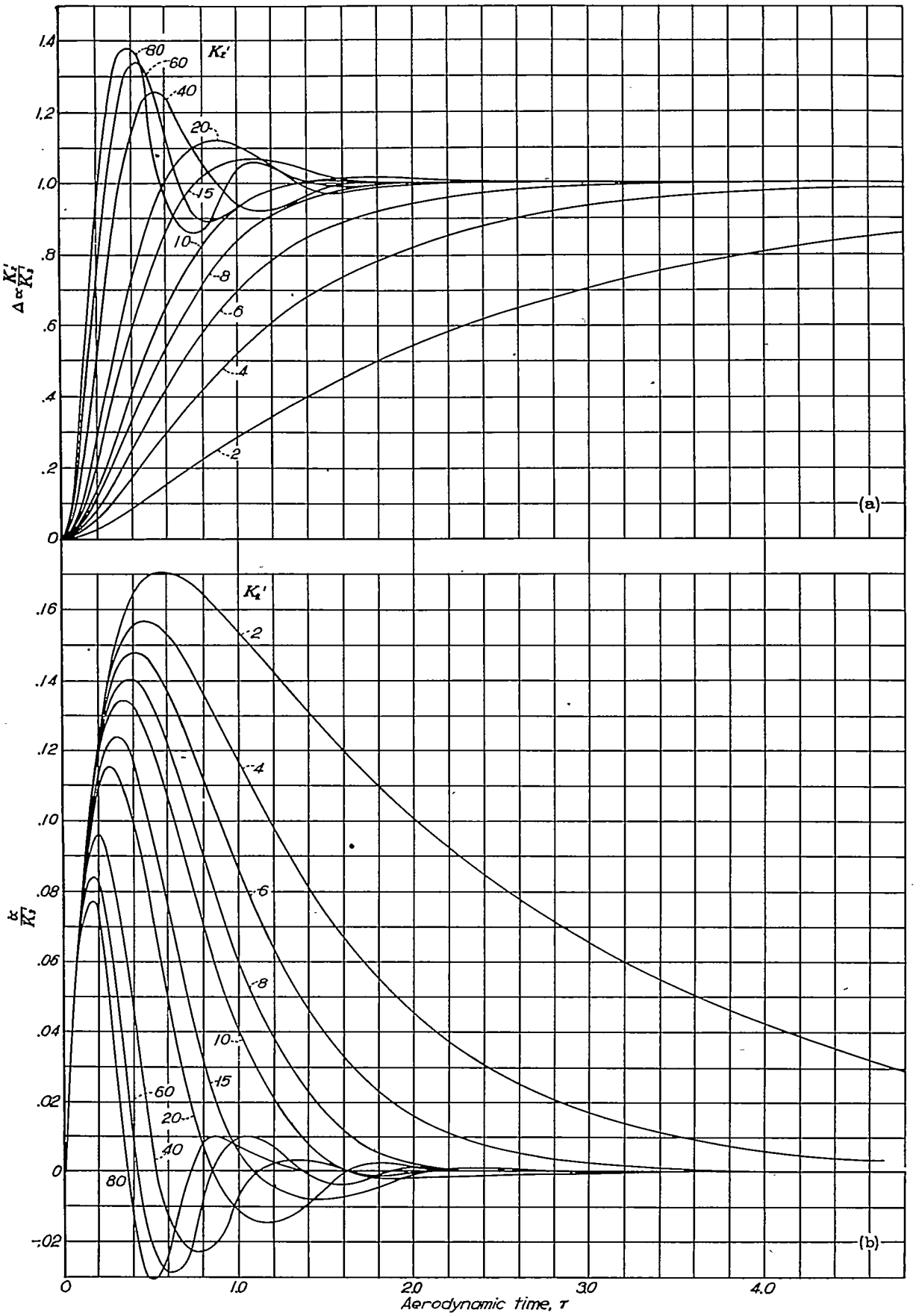

FIGURE 2—Variation of $\Delta\alpha\frac{K_1'}{K_2'}$ and $\frac{\dot{\alpha}}{K_2'}$ with aerodynamic time for an instantaneous elevator deflection. $K_1'=5.0$.

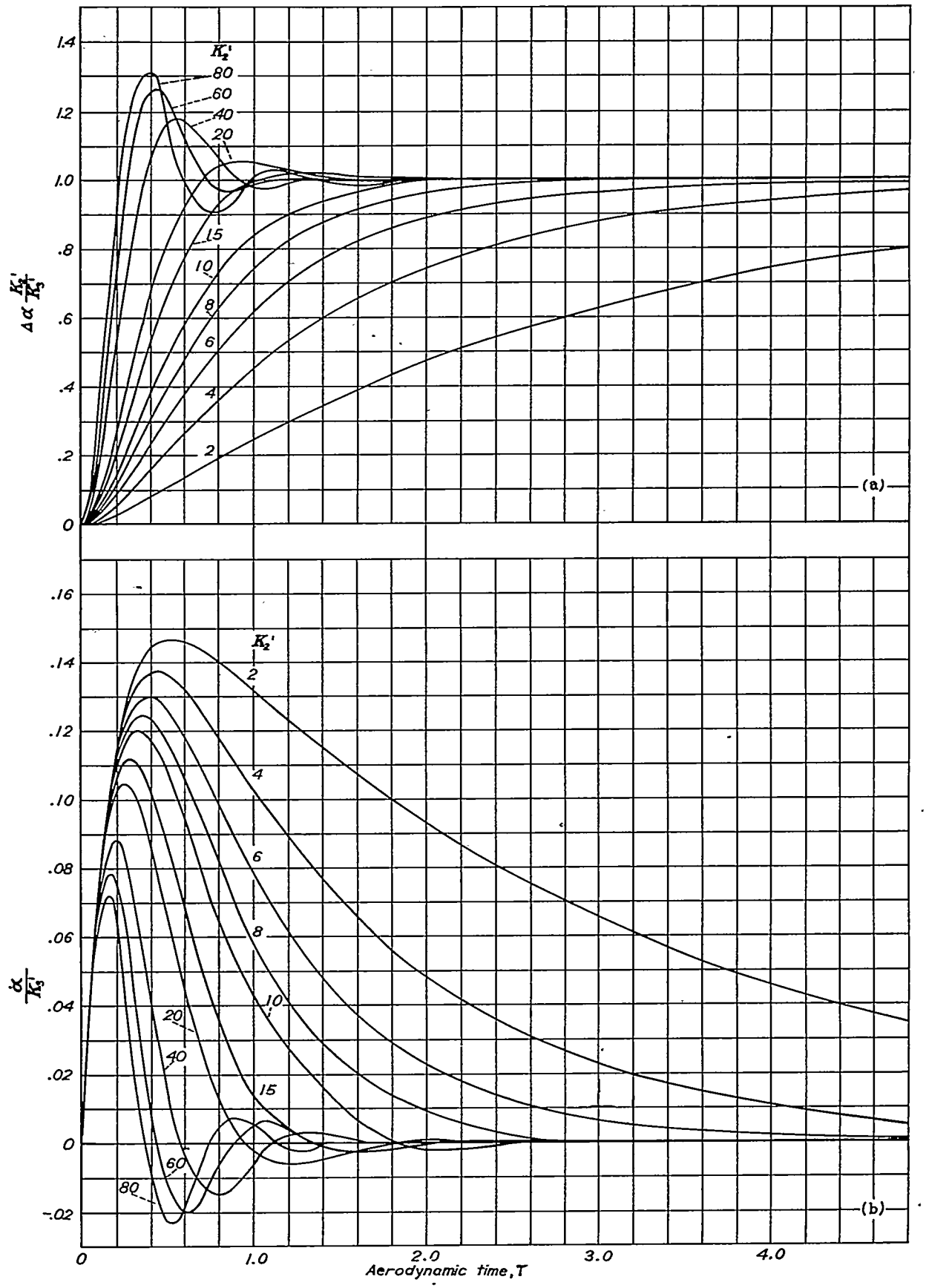

FIGURE 3.—Variation of $\Delta\alpha \frac{K_2'}{K_3'}$ and $\frac{\dot{\alpha}}{K_3'}$ with aerodynamic time for an instantaneous elevator deflection. $K_1' = 6.0$.

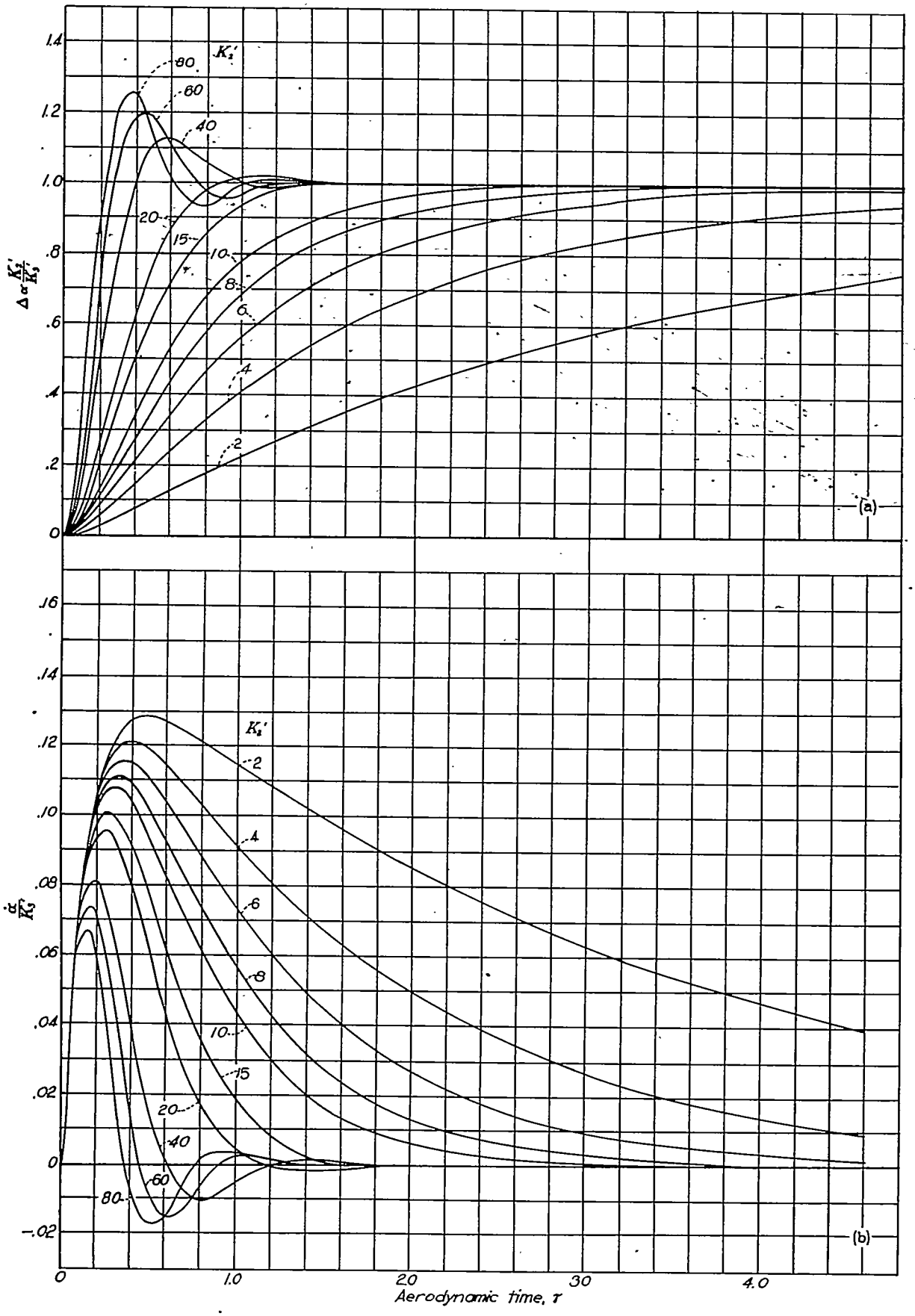

FIGURE 4.—Variation of $\Delta\alpha\frac{K_1'}{K_3'}$ and $\frac{\dot{\alpha}}{K_3'}$ with aerodynamic time for an instantaneous elevator deflection. $K_1'=7.0$.

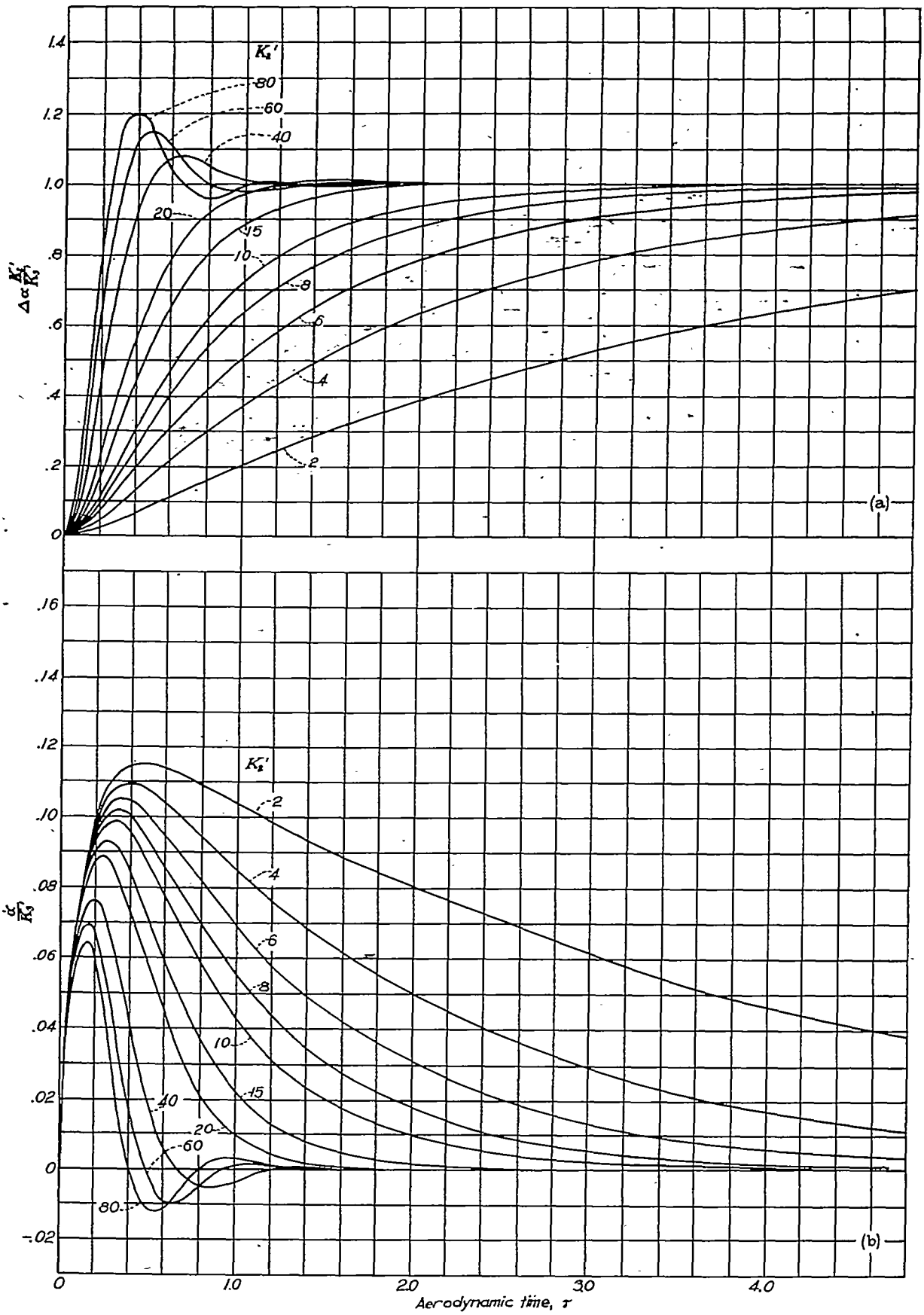

FIGURE 5.—Variation of $\Delta\alpha\frac{K_2'}{K_3'}$ and $\frac{\dot{\alpha}}{K_3'}$ with aerodynamic time for an instantaneous elevator deflection. $K_1'=8.0$.

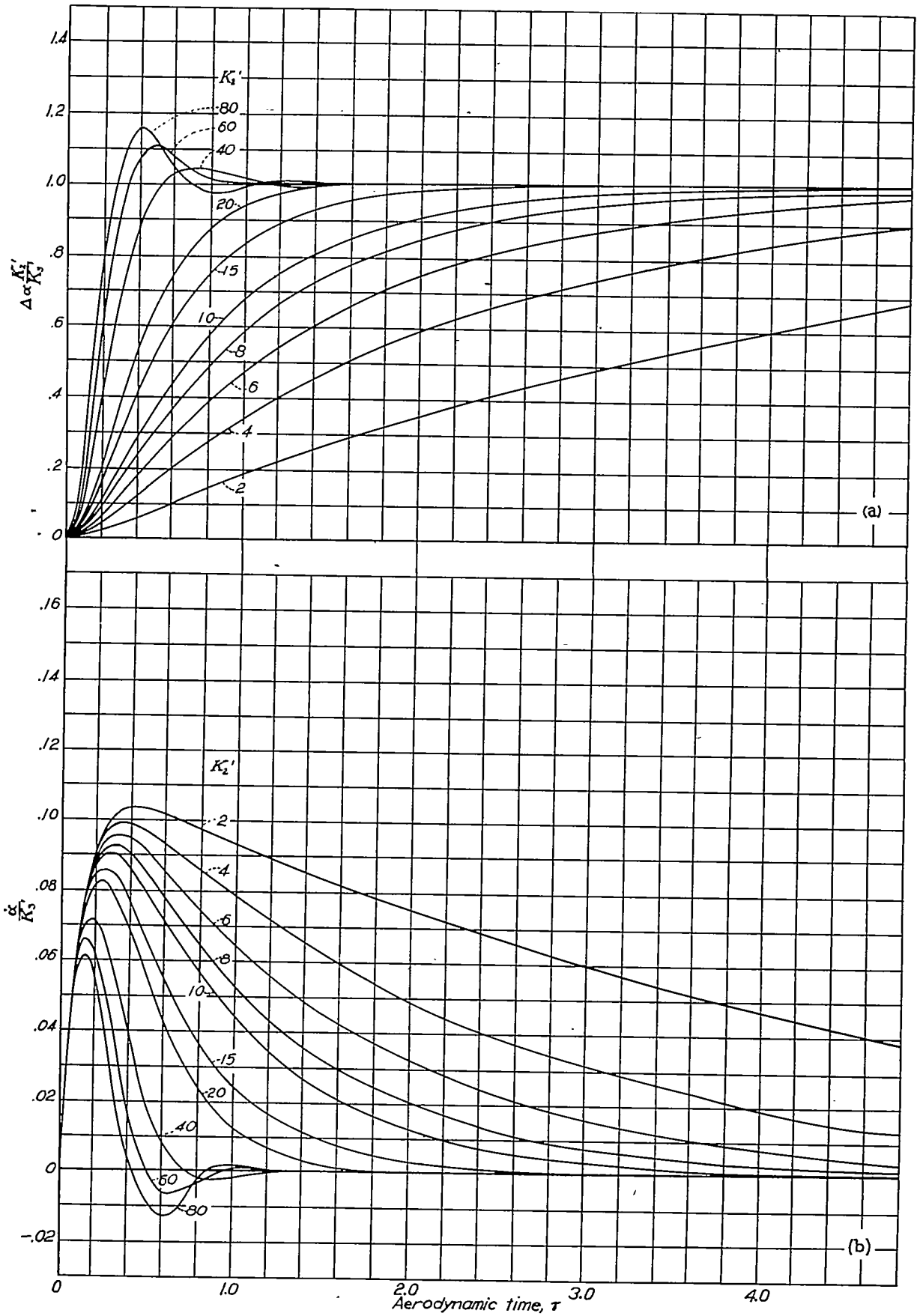

FIGURE 6.—Variation of $\Delta\alpha\frac{K_2'}{K_3'}$ and $\frac{\dot{\alpha}}{K_3'}$ with aerodynamic time for an instantaneous elevator deflection. $K_1'=9.0$.

The necessary geometric and aerodynamic characteristics of this airplane are as follows:

GEOMETRIC

Gross wing area, S, square feet	300
Gross horizontal tail area, S_t, square feet	60
Airplane weight, W, pounds	12,000
Wing span, b, feet	41
Tail span, b_t, feet	16
Radius of gyration, k_Y, feet	6.4
Distance from aerodynamic center of airplane less tail to aerodynamic center of tail, x_t, feet	−21.0

AERODYNAMIC

Slope of airplane lift curve, $\frac{dC_L}{d\alpha}$, radians	4.87
Slope of tail lift curve, $\frac{dC_{L_t}}{d\alpha_t}$, radians	3.15
Downwash factor, $d\epsilon/d\alpha$	0.54
Tail efficiency factor (q_t/q), η_t	1.00
Empirical airplane damping factor, K	1.1
Elevator effectiveness factor, $\frac{dC_{L_t}}{d\delta}$, radians	1.89
Rate of change of tail moment with camber due to elevator angle, $\frac{dC_{m_t}}{d\delta_t}$, radian	−0.57
Rate of change of moment coefficient with angle of attack:	
(a) center of gravity, 30 percent, radian	0.703
(b) center of gravity, 25 percent, radian	0.475

It was determined from tests of this airplane that for the conditions desired the slope of the moment curve per radian for the airplane less tail could be given by $\frac{dC_m}{d\alpha}=-0.665+0.0445\ c.\ g.$

Substitution of the geometric and aerodynamic values into equation (15a) and the assumption that results are required for an altitude of 19,100 feet ($\rho=0.001306$) give the following values for K_1', K_2', and K_3':

$$K_1'=8.0$$

$$K_2'\ (c.\ g.\ \text{at 30 percent})=20.0$$

$$K_2'\ (c.\ g.\ \text{at 25 percent})=40.0$$

$$K_3'=-100.0$$

For these values of K_1' and K_2', the variation of $\Delta\alpha\frac{K_2'}{K_3'}$ and $\frac{\dot{\alpha}}{K_3'}$ with τ can be obtained from figures 5(a) and 5(b) for an instantaneous unit elevator deflection. A slight amount of labor can be saved at this stage if the curves are taken directly from these figures onto a work sheet (see middle group of curves in fig. 7) without transforming them into curves of $\Delta\alpha$ and $\dot{\alpha}$. The transformation can, of course, be accomplished immediately by multiplying the ordinates of the curves obtained by $\frac{K_3'}{K_2'}$ and K_3', respectively. It has been found more convenient, however, to make the change-over as a final step.

The next step in the procedure is to plot the assumed elevator-motion curve on the work sheet using the same abscissa (τ). This change is accomplished by dividing the actual assumed time variation of elevator deflection by the factor $m/\rho SV$ in order to obtain the variation in aerodynamic units. For an indicated speed of 400 miles per hour at 19,100 feet, the factor $m/\rho SV$ for the airplane in question would be $\frac{W/S}{(g\rho)V\sqrt{\rho_0/\rho}(88/60)}=\frac{40}{0.0420\times400\times1.349\times1.466}=1.202$ seconds.

The determination of $\Delta\alpha\frac{K_2'}{K_3'}$ and $\frac{\dot{\alpha}}{K_3'}$ at any time τ due to the assumed elevator motion is then found by the following graphical construction. This construction is essentially that given in reference 2 except for minor modifications that were found to be worth while in effecting the computations. The values of $\Delta\alpha\frac{K_2'}{K_3'}$ and $\frac{\dot{\alpha}}{K_3'}$ at the aerodynamic time $\tau_0=1$, for example, due to the assumed elevator motion are found as follows:

1. First, the point on the $\Delta\delta$ curve at $\tau=1$ is projected horizontally in both directions until it strikes the 45° lines. The intersections with these lines are then projected or deflected vertically until they intersect the horizontal projections of the values of $\frac{\dot{\alpha}}{K_3'}$ and $\Delta\alpha\frac{K_2'}{K_3'}$ at the time τ equal to zero. The points labeled ① are thus established.

2. The ordinate of the $\Delta\delta$ curve at, say, $\tau=0.8$ is next projected horizontally as before until it strikes the 45° lines, where it is reflected and points of intersection with the horizontal projections of the values of $\Delta\alpha\frac{K_2'}{K_3'}$ and $\frac{\dot{\alpha}}{K_3'}$ at $\tau=0.2$ second are established. The points labeled ② are obtained in this manner. Other points labeled ③ to ⑤ for $\tau=0.2$, 0.1, and 0 are then similarly obtained to complete the curve for the example chosen and for the time $\tau_0=1.0$. Note that the addition of τ on the elevator curve and τ on the unit-function curve always equals τ_0. Curves are then drawn through these points and the areas under them are proportional to $\Delta\alpha$ and $\dot{\alpha}$ for the aerodynamic time of 1 unit.

3. The areas are found by integrating in the direction shown, that is, ⓪, ①, ②, ③, and so forth. It is important to follow in this direction in order that negative areas, if they should occur, may be properly taken into account. If the points are followed in the order noted and a counterclockwise path is followed in enclosing the area, the value is positive regardless of the quadrants involved and vice versa for clockwise integration. When a figure-of-eight area is involved, the same statement also applies. The areas are then converted to $\Delta\alpha$ and $\dot{\alpha}$ by multiplying the number of square units (square inches or square centimeters) by the appropriate conversion factors, which are obtained by multiplying the ordinate scales of $\Delta\alpha$ or $\dot{\alpha}$ by the ordinate scales of $\Delta\delta$ curves as the case may be.

4. Other curves are similarly drawn in for the different time intervals, τ_0, at which the values of $\Delta\alpha$ and $\dot{\alpha}$ are desired. For example, see the curve drawn in for the time $\tau_0=2.2$ with points labeled [1], [2], and so forth.

5. After a sufficient number of time intervals are considered and the resulting areas determined, the final step is to convert the areas into the values of $\Delta\alpha$ and $\dot{\alpha}$ associated with the elevator motion assumed. The variation of load factor and tail-load increment may then be found by substituting for $\Delta\alpha$ and $\dot{\alpha}$ into equations (12), (13), and (14). It is convenient at this stage to arrange the results in tabular form and to convert from time τ to time t.

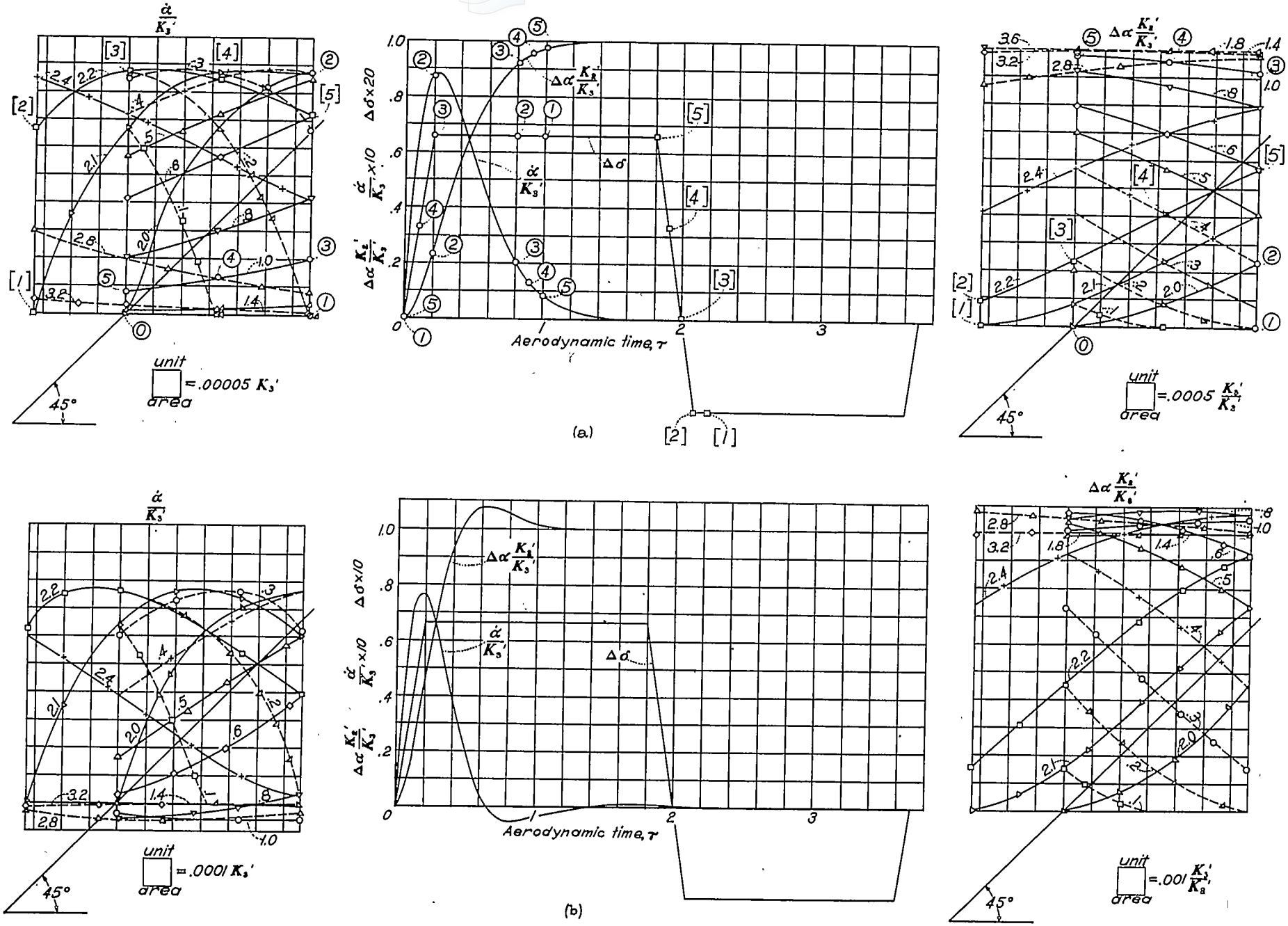

(a) $K_1'=20.0$.

(b) $K_1'=40.0$.

FIGURE 7.—Determination of $\Delta\alpha$ and $\dot{\alpha}$ for the elevator motion suggested in reference 1. $K_1'=8.0$; $K_2'=-100.0$.

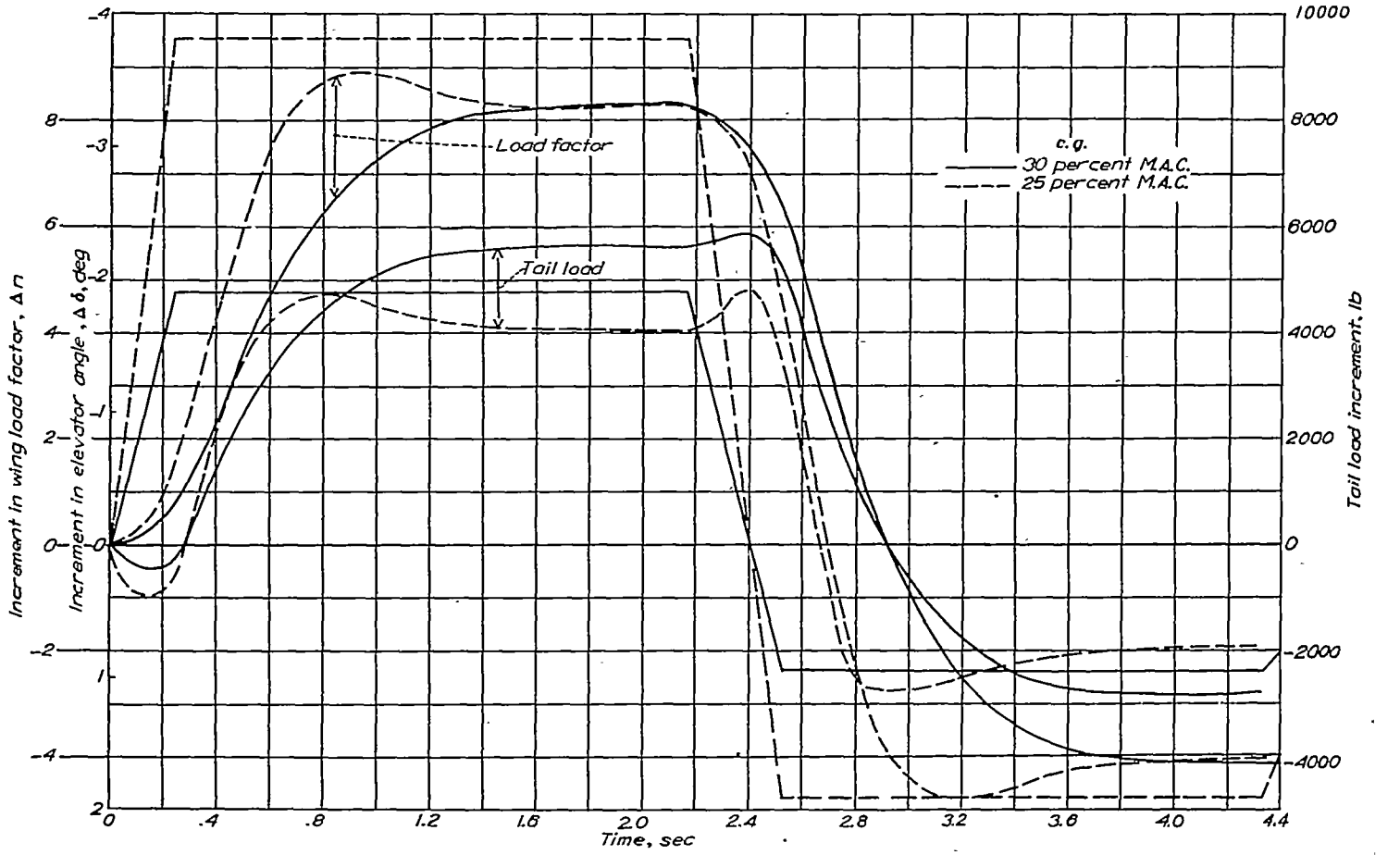

FIGURE 8.—Load variation for examples of figure 7.

Figure 8 gives the final variation of the load factor and tail-load increments for the example of figure 7. The type of elevator motion used in these figures is that previously suggested in reference 1 in which the horizontal tail would be designed to withstand a maneuver in which the V–G diagram from maximum positive to maximum negative g would be covered. The duration of the time intervals at which the elevator was held at maximum values $\pm\Delta\delta_{max}$ was adjusted so that the full acceleration corresponding to each elevator throw would be reached. The rates of movement were purposely taken quite high in order to obtain as large downtail or control loads as possible without exceeding the speed at which the pilot might move the controls. The relation between the elevator throw $\Delta\delta_{max}$ and the load factor increment Δn that is finally reached is given by

$$\Delta\delta_{max}=\Delta n\frac{K_2'}{K_3'}\frac{W/S}{\frac{dC_L}{d\alpha}q}$$

This relation is easily obtained by substituting the values for $\Delta\alpha$ from equations (16) (with t large) into equation (12).

In order to obtain this range in acceleration, it is not necessary that the pilot restrict himself to the type of elevator motion assumed, as he may actually move the elevator twice as far as is necessary and check the motion earlier so as not to overshoot the desired acceleration. Such a motion is illustrated by the results given in figures 9 and 10 for the same airplane (K_1'=8, K_2'=20) but with the elevator motion required to cover approximately the same acceleration range.

It will be noted in figure 10 that the maximum acceleration reached with the elevator motion assumed was 8.75g instead of 8g. A number of trial computations made in connection with the figure indicated that, other things being equal, a delay of as little as 0.06 second in the time of the elevator reversal would cause the acceleration to overshoot by 1.5g. This delay indicates that the particular type of elevator motion shown in figure 10 would probably never be used by a pilot in a high g pull-out and where the elevator motion is small because of the extremely fine timing required to prevent overloading.

Comparison of the results of figure 10 with those of figure 8 for the same values of K_2' indicates a much more rapid variation in load factor for the type of motion used in figure 10. Jones and Fehlner, in reference 3, have shown that the transient effects of wing wake on the tail are likely to be severe only when the rate of change of wing angle of attack is great. These effects are not included in the method given because in the usual case they apparently are of little importance in the determination of the critical-maneuver tail load. In order to illustrate the combined effects of aerodynamic lag and transient wing wake on tail loads, a portion of the tail-load curve in the critical region, including transient effects, has been computed by R. T. Jones for the case illustrated in figure 10. The comparison is given in figure 11 where it will be seen that even in this particularly severe case the discrepancy amounts to only about 10 percent on the important maximum loads.

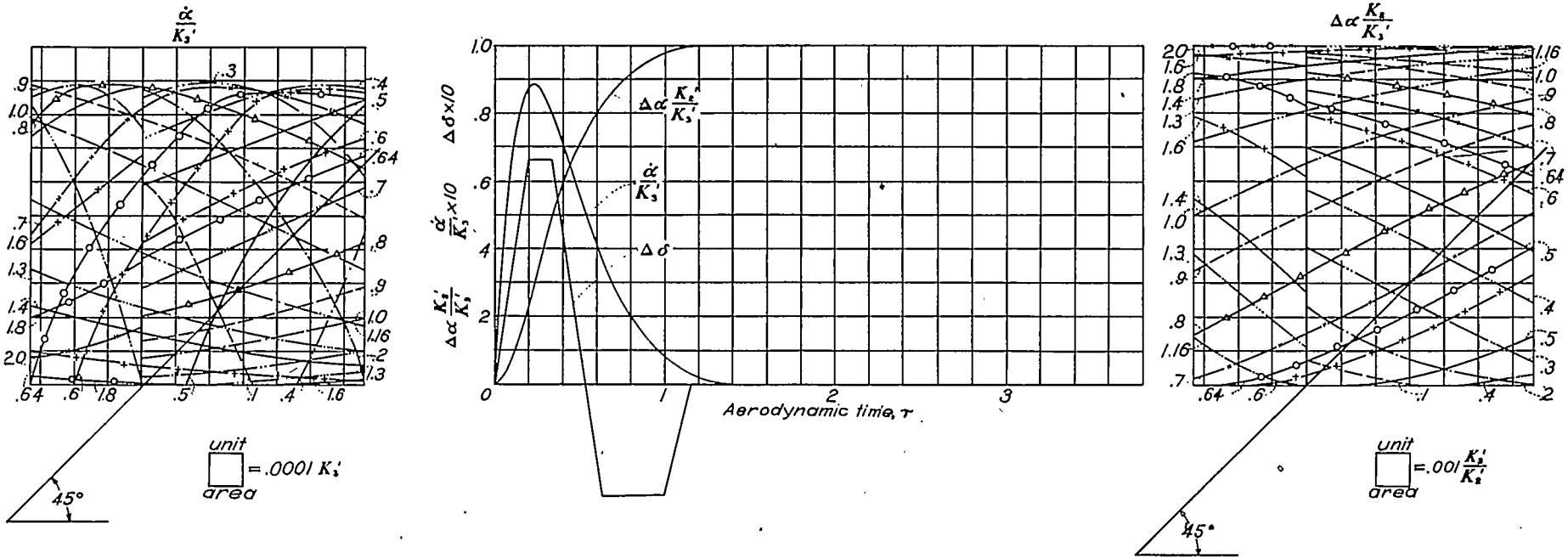

FIGURE 9.—Determination of $\Delta\alpha$ and $\dot{\alpha}$ for rapid reversal of elevator. $K_1'=8.0$; $K_2'=20.0$; $K_3'=-100.0$.

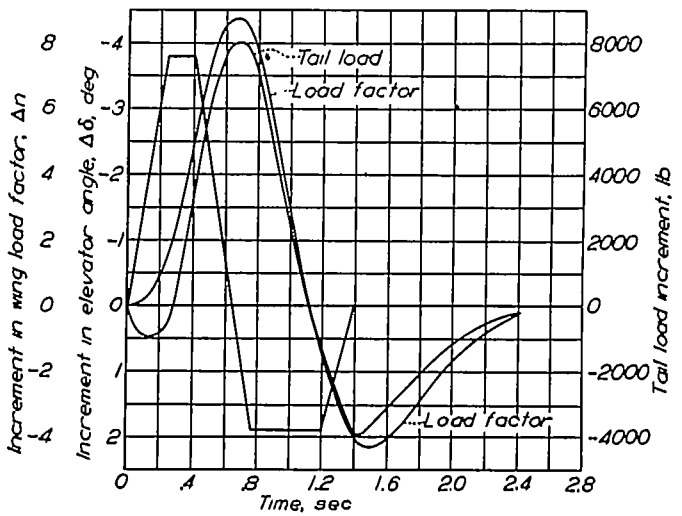

FIGURE 10.—Load variation for example of figure 9. Center of gravity, 30 percent M. A. C.

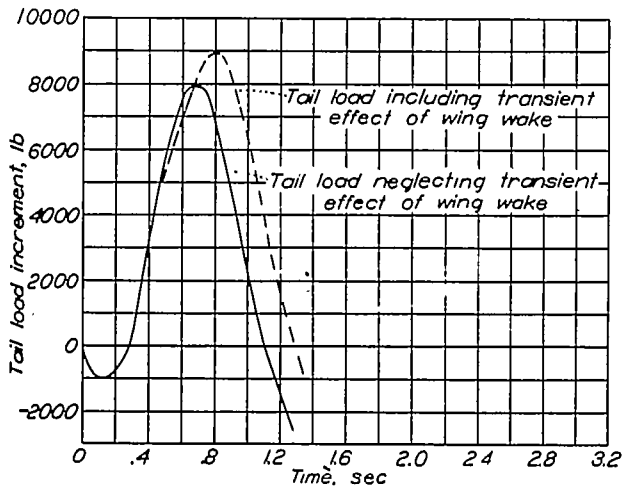

FIGURE 11.—Effect of transient wing wake on the tail load.

Because actual elevator motions are almost certain to be less severe than the one illustrated, the transient effect will be less than that shown and within the limits of accuracy with which some items entering into the computations are known. For this reason, and because of the increased mathematical complexity that is introduced by its inclusion, transient effects are omitted. This statement, however, cannot be assumed to apply to the gust condition wherein the angle-of-attack changes may occur more rapidly.

POSSIBLE SHORT CUTS

The preceding section illustrated a general procedure that can be followed where one or two elevator motions are to be investigated, but there are a number of variations which might have been used. If, however, the effects of a fairly large number of elevator motions are to be investigated at a given speed and altitude, the following method can be used with a saving in time.

1. Determine a unit tail load ΔL_t and wing load Δn directly by using values of $\dot{\alpha}$ and $\Delta\alpha$ obtained from figures 2 to 6 and substituting these values into equations (12) and (14).

2. Plot the values Δn and ΔL_t of step 1 as a function of time instead of plotting $\Delta\alpha$ and · as a function of time as in figures 7 and 9.

3. Plot the elevator-motion curve to be investigated and proceed as before. The areas now obtained will give directly the increments of tail load and wing load.

A quicker method of obtaining the areas, in some cases, and one that is readily apparent after a little experience is gained, is to prepare grids for evaluating either $\Delta\alpha$ and $\dot{\alpha}$ or Δn and ΔL_t. The abscissas of the vertical lines of the grids are simply the ordinates of the considered elevator-motion curve taken every 0.1 or 0.2 second, say; the ordinates of the horizontal lines of the grid are then the ordinates of the respective unit curves. Figure 12 shows such a grid for determining $\Delta\alpha\frac{K_2'}{K_3'}$ for the conditions of figure 7(a). In order to obtain the value of $\Delta\alpha\frac{K_2'}{K_3'}$ for the specific time of τ_0=1.0, the points of intersection of the horizontal and vertical grid lines adding up to 1.0 are connected. Such a curve is shown in figure 12 for comparison with the similar one given in figure 7(a).

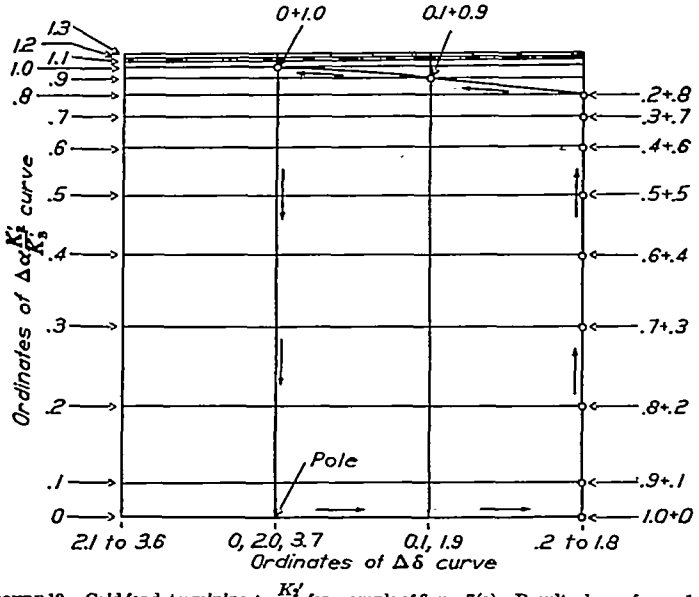

FIGURE 12.—Grid for determining $\Delta\alpha\frac{K_2'}{K_3'}$ for example of figure 7(a). Results shown for τ_0=1.0.

DETERMINATION OF THE NECESSARY AERODYNAMIC DERIVATIVES

The accuracy with which the load increments may be determined for a given elevator motion depends largely upon the accuracy with which certain aerodynamic characteristics are known and, in some measure, on how well these characteristics may be approximated by a straight line. The values required for the computation may be obtained with sufficient accuracy from wind-tunnel tests of a model in which the lift, drag, and moment are measured with and without the tail in place and with the power condition for which calculations are to be made. Lift and moment measurements should also be made for a range of elevator angles from $\pm 10°$; then, with elevator fixed, the lift and moment variation with tail setting should be determined through a range of about 5°.

The value of $dC_L/d\alpha$ to be used should be that obtained with the tail in place and should be based on the gross wing area. By the use of this value, most of the effect of tail load on normal acceleration will be taken into account.

The value of $dC_m/d\alpha$ to be used is the slope of the moment curve with the horizontal tail removed. Usually, the moment variation is taken with respect to a selected center-of-gravity position, but it is desirable that the variation of $dC_m/d\alpha$ with center-of-gravity position be determined for at least two center-of-gravity positions. For the conventional fighter airplane it appears that the critical total down load at the tail will occur with the center of gravity in its most forward position during dive pull-outs at high altitude and at the limiting speed. The maximum up-load at the tail is likely to occur during pull-ups from high-speed level flight with the center of gravity in its most rearward position and at a relatively low altitude.

The value of the factor $\eta_t\frac{dC_{L_t}}{d\alpha_t}$ can be obtained from moment differences obtained at the same angle of attack from two settings i_t of the horizontal tail plane. Thus,

$$\eta_t\frac{dC_{L_t}}{d\alpha_t}=\frac{\Delta C_{m_{ac}}S^2}{\Delta i_t b S_t x_t}$$

It will not generally be necessary to separate the factor η_t but this separation could be accomplished by reference to tests of isolated tail surfaces of a similar plan form. Reference 4 gives results for tests of a number of isolated tail surfaces.

The previous value obtained for $\eta_t\frac{dC_{L_t}}{d\alpha_t}$ can be used to find the elevator effectiveness $d\alpha_t/d\delta$ or $\frac{dC_{L_t}}{d\delta}$ from either the moment or the lift differences obtained from tests in which the elevator angle was varied.

Moment differences

$$\frac{d\alpha_t}{d\delta}=\frac{\Delta C_{m_{av}}S^2}{\eta_t\frac{dC_{L_t}}{d\alpha_t}S_t x_t b\Delta\delta}$$

$$\eta_t\frac{dC_{L_t}}{d\delta}=\frac{\Delta C_{m_{av}}S^2}{S_t x_t b\Delta\delta}$$

Lift differences

$$\frac{d\alpha_t}{d\delta}=\frac{\Delta C_{L_{av}}S}{\eta_t\frac{dC_{L_t}}{d\alpha_t}S_t\Delta\delta}$$

$$\eta_t\frac{dC_{L_t}}{d\delta}=\frac{\Delta C_{L_{av}}S}{S_t\Delta\delta}$$

The differences ΔC_L and ΔC_m are to be taken at the same angle of attack. In general, the moment differences will prove to be the most reliable because the quantities involved are larger.

Similarly, the downwash factor can be determined on the basis of either moment or lift differences with and without the tail in place together with the previous value obtained for $\eta_t\frac{dC_{L_t}}{d\alpha_t}$

Moment differences

$$\left(1-\frac{d\epsilon}{d\alpha}\right)=\Delta\left(\frac{dC_m}{d\alpha}\right)\frac{S^2}{S_t b x_t}\cdot\frac{1}{\eta_t\frac{dC_{L_t}}{d\alpha_t}}$$

where $\Delta\left(\frac{dC_m}{d\alpha}\right)$ is the increment in the slope $\left(\frac{dC_m}{d\alpha}\right)$ caused by the addition of the tail.

Lift differences

$$\left(1-\frac{d\epsilon}{d\alpha}\right)=\frac{S}{S_t\eta_t\frac{dC_{L_t}}{d\alpha_t}}\left[\left(\frac{dC_L}{d\alpha}\right)_{\text{tail on}}-\left(\frac{dC_L}{d\alpha}\right)_{\text{tail off}}\right]$$

The values obtained from the moment differences are the more reliable.

LANGLEY MEMORIAL AERONAUTICAL LABORATORY,
NATIONAL ADVISORY COMMITTEE FOR AERONAUTICS,
LANGLEY FIELD, VA., *November 23, 1942.*

REFERENCES

1. Pearson, H. A., and Garvin, J. B.: An Analytical Study of Wing and Tail Loads Associated with an Elevator Deflection. NACA ARR, June 1941.
2. Jones, Robert T.: Calculation of the Motion of an Airplane under the Influence of Irregular Disturbances. Jour. Aero. Sci., vol. 3, no. 12, Oct. 1936, pp. 419–425.
3. Jones, Robert T., and Fehlner, Leo F.: Transient Effects of the Wing Wake on the Horizontal Tail. NACA TN No. 771, 1940.
4. Silverstein, Abe, and Katzoff, S.: Aerodynamic Characteristics of Horizontal Tail Surfaces. NACA Rep. No. 688, 1940.